

A microchopper for neutral beams

K. Kuhnke,^{a)} K. Kern,^{a)} R. David, B. Lindenau, and G. Comsa
*Institut für Grenzflächenforschung und Vakuumphysik, KFA-Forschungszentrum Jülich,
Postfach 1913, D-52425 Jülich, Germany*

(Received 25 October 1993; accepted for publication 3 December 1993)

A mechanical beam chopper with small dimensions is presented. The shape of the generated neutral beam pulses is calculated and experimental results are discussed. The microchopper is based on the operation principle of neutron choppers. It is operated in vacuum and generates molecular beam pulses at a repetition rate of 10 kHz with pulse lengths easily adjustable between 5 and $< 1 \mu\text{s}$. The chopper can be used for time-of-flight applications and inherently acts as a high velocity pass filter.

I. INTRODUCTION

Molecular beam choppers are a standard tool to provide short pulses for energy analysis or monochromatization (time-of-flight technique). A wide variety of concepts can be found in the literature.¹⁻⁵ Vibrating slit choppers, for example, can be built very small. They generate pulse lengths down to about $150 \mu\text{s}$.¹ The pulse length is determined by the time it takes the slit to cross the beam. The ultimate limitation for a chopper is the mechanical stability during the deceleration and acceleration at the turning points of the oscillatory motion. The mechanical stability can be pushed to its limits by using the continuous acceleration of rotating disc choppers. Pulse lengths of $2.5 \mu\text{s}$ are typically obtained with slits of 0.75 mm width on the circumference of a rotating disk with 244 mm diameter, rotating at a frequency of 400 Hz.⁴ Under these operational conditions the limit of stability is already reached for alloys like copper-beryllium, which provides a favorable relation between tensile strength and specific weight.⁴ The slit width cannot be reduced substantially without loss of mechanical precision.

In this article we present the design and the properties of a different type of neutral beam chopper and demonstrate its operation. The device has the virtues of a high precision conventional rotating disk chopper. In addition it allows a simple and fast change of pulse lengths down to less than $1 \mu\text{s}$ with a duty cycle as high as 1:100. Conventional choppers near $1 \mu\text{s}$ have large dimensions (typical disk diameters of 250 mm). In contrast, the active part of our device is a spinning rotor, 5.6 mm in diameter, and the whole chopper assembly fits completely into a cylinder of 70 mm diameter centered on the beam. It has a total length of 45 mm along the beam axis. The chopper is based on the design of the spinning rotor pressure gauge.⁶ Its principle of operation is similar to the one of neutron choppers.⁷

The microchopper was developed in order to directly measure the time resolution of a He ionization detector ($1.5\text{--}4 \mu\text{s}$ range). This application establishes the necessity of extremely short pulse lengths and unusually small dimensions.⁸

^{a)}Present address: Institut de Physique Experimentale, EPFL, CH-1015 Lausanne; Switzerland.

II. CHOPPER DESIGN

A spinning cylinder (rotor) is magnetically suspended inside an evacuated tube in the path of a neutral (e.g., molecular) beam. A hole drilled perpendicular to the rotational axis permits beam passage for short intervals and thus generates the particle pulses. Figure 1(a) shows the setup that employs a spinning rotor gauge (SRG) head which embraces the evacuated tube, 9 mm in diameter (wall thickness 0.2 mm). The SRG head must be under atmospheric pressure to provide sufficient cooling of the coils. The head cannot be removed from the tube when under vacuum. Therefore the bakeout temperature is limited to some 60°C . The SRG head is identical to the one used for the commercial spinning rotor gauge.⁶ We use two electronic supply units which are prototypes of components of the commercial device: one unit controls the active magnetic suspension, the other unit supplies the ac current for the rotating magnetic field that accelerates the rotor. By exchanging a condensator, the output frequency of the latter unit is changed from about 400 Hz (used in the original spinning rotor gauge) to 10 kHz. The rotor can thus be asynchronously accelerated to a rotation frequency close to 10 kHz. When the rotor approaches its operation frequency, the accelerating field is turned off. During the ensuing "free drift" phase, the chopper is ready to provide neutral beam pulses. With the acceleration field turned off, two coils in the SRG head pick up the signal of the rotors spinning magnetic moment and thus provide a signal that is synchronous with the pulse generation and which is needed for time-of-flight applications. In the signal from the pickup coils an interfering frequency of 33 kHz is suppressed by a low pass filter [see Fig. 1(a)]. The synchronous transistor-transistor logic (TTL) signal is then generated by a Schmitt trigger after the 5 mV sinusoidal pickup signal has been excessively amplified (by a factor of $> 10^5$) to obtain a step function. As synchronous pulse and beam pulse are generated with a certain phase shift, the gradual deceleration during the free drift of the rotor continuously changes the time between synchronous signal and particle pulse. The deceleration determines the interval (usually several minutes to an hour) in which a single measurement must be accomplished in order not to lose the choppers time resolution. The use of a tunable acceleration frequency may provide an alternative operation

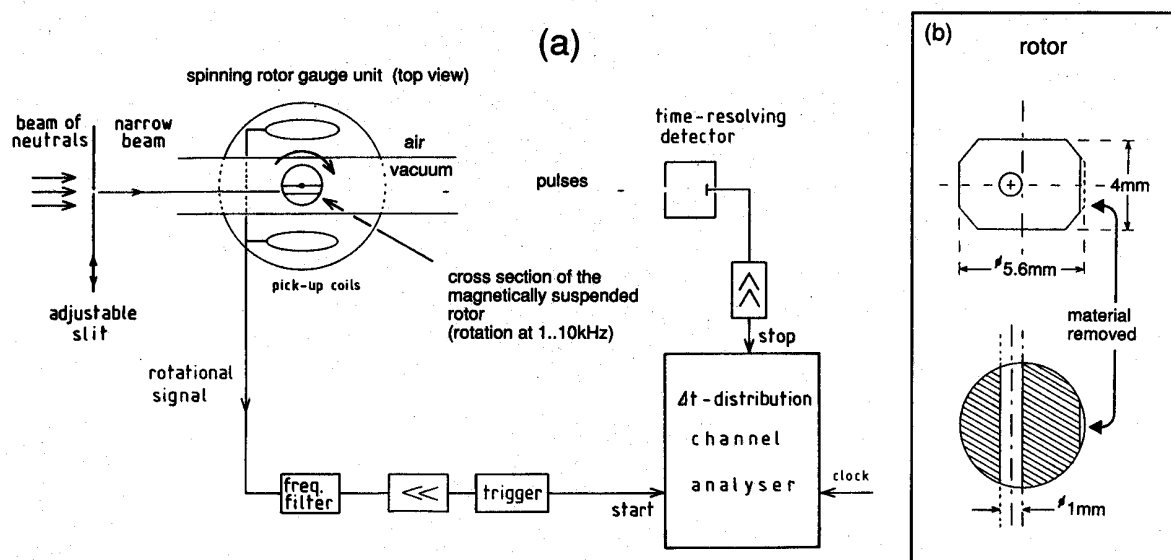


FIG. 1. (a) Microchopper setup for time-of-flight experiments. A narrow slit reduces the lateral beam dimension to a thin slice, which passes through the bore hole in the magnetically suspended spinning rotor. A synchronous signal starts a clock, which is stopped by a measured particle in the detector. The distribution of flight times is displayed in the multichannel analyzer. (b) Rotor design with the cylindrical bore hole which chops the neutral particle beam.

mode in which the rotor could be driven synchronously at 10 kHz and the synchronization signal can be derived from the driving frequency. This mode allows a permanent chopper operation. However, it would require some electronic modifications.

The design of the cylindrical/conical rotor is shown in Fig. 1(b). Positioning the bore hole off the center of the rotor avoids the generation of a second pulse with different characteristics during the same revolution. Material is removed on the opposite side to keep the inertial axis centered. The rotational axis is the axis with the largest moment of inertia.

The rotor is made of magnetic steel that has a tensile strength of 10^9 Pa (at 0.2% plastic deformation). For safety reasons the steel was not hardened, so that slow plastic deformation of the rotor would occur rather than sudden disintegration. The maximum tensile strain at a rotation frequency of 10 kHz was estimated to be 4×10^8 Pa. It is effective in the center of the rotor above and below the bore hole.⁹

III. PULSE PROPERTIES

The characteristics of the pulses generated by the passage of the beam through the bore hole of the microchopper are calculated for a simplified geometry. The rotating bore hole is reduced to an entrance pinhole and an exit pinhole moving on a straight line perpendicular to the beam direction. This approximation is valid, because (a) the diameter of the bore hole is much smaller than the diameter of the rotor, (b) the bore hole passes close to the center of the rotor, and (c) molecules hitting the inner surface of the bore hole are removed from the beam.¹⁰ In a first approach we further simplify the geometry to two dimensions not taking into account that for the cylindrical

bore hole the slit width in Fig. 2 is a function of the distance from the equator of the rotor: $d = d(y)$. Assuming a monochromatic beam of particles of velocity v , the first moving slit allows the passage of a diagonal strip of particles. This region of passing particles travels to the second slit where it intersects with the diagonal strip that represents the pass conditions for the second slit. The field of transmitted particles has the shape of a truncated rhomb [Fig. 3(a)] or, for slower particles, the shape of a triangle [Fig. 3(b)]. Particles with a velocity $v < R^2\omega/d$ are completely blocked from passage. Here, R is the radius of the rotor, ω its angular velocity, and d the diameter of the bore hole. The pulse duration τ at a given x coordinate is

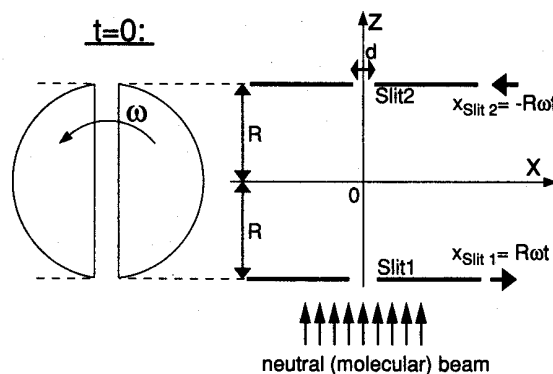


FIG. 2. Approximation of the chopper geometry by two slits moving on straight lines with constant velocities. R is the radius of the rotor at its equator, ω its angular velocity, and d the diameter of the bore hole. The x axis is defined as the direction perpendicular to both rotor axis and beam direction.

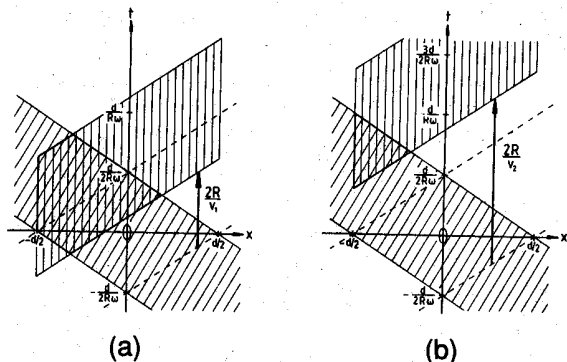


FIG. 3. The shape of the passing pulse in x, t coordinates is the intersection of two strips representing the pass conditions of slit 1 and slit 2. The two strips are shifted with respect to each other by the time it takes a particle to travel the distance between the slits. For beam velocities $v > 2R^2\omega/d$ (a) the pulse has the shape of a truncated rhomb, for $R^2\omega/d < v < 2R^2\omega/d$ (b) the pulse has triangular shape.

$$\tau(x) = \begin{cases} \frac{d}{R\omega} \left(1 - \frac{2}{d} \left| x + \frac{R^2\omega}{v} \right| \right), & \text{if } -\frac{d}{2} < x < \frac{d}{2} - \frac{R^2\omega}{v} \\ 0, & \text{else.} \end{cases} \quad (1)$$

A graphical representation of Eq. (1) is given in Fig. 4. For a broad velocity distribution of the particles in the beam, the chopper acts as a velocity high pass filter.

Due to its dependence on the x coordinate [Eq. (1)] the pulse duration can be adjusted by choosing the position, where the beam passes through the pinholes. In practice this can be simply done by adjusting a narrow slit in front of the rotor [Fig. 1(a)], or behind the rotor.

For the channel geometry (Fig. 2 left hand side) Eq. (1) is not strictly correct for all coordinates $x < 0$. Some particles that have passed slit 1 and would also pass slit 2 hit the wall of the channel (the left hand side wall in Fig.

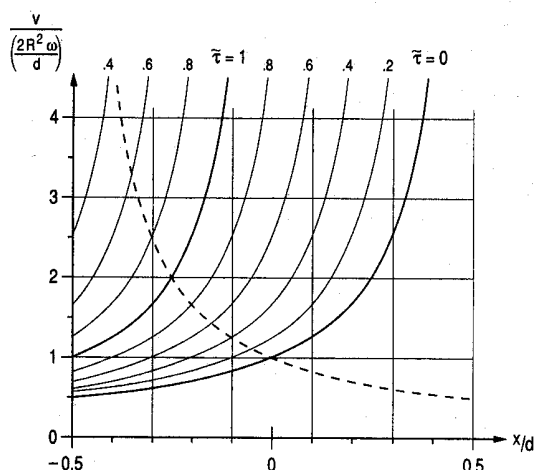


FIG. 4. Pulse length $\bar{\tau}$ as a function of position x and beam velocity v for the geometry of Fig. 2. The absolute pulse length in seconds is obtained as $\tau = (d/R\omega)\bar{\tau}$. For the realistic geometry in which the two pinholes are connected by a channel, the result predicts too long pulse lengths on the left of the broken line (see text). The difference between the indicated pulse width and the true one is zero on this line and increases to the left.

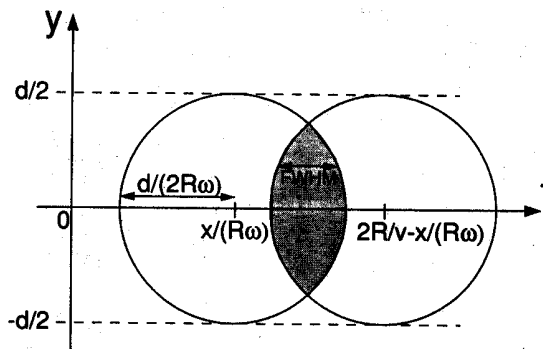


FIG. 5. The shape of the passing pulse generated by a cylindrical bore hole in y, t coordinates is the intersection of two ellipses. The y axis is parallel to the rotation axis of the rotor.

2). This happens at all coordinates $x < -(d/2) + (R^2\omega/v)$, thus reducing the pulse length with regard to Eq. (1) (see also Fig. 4). For the three-dimensional problem of the cylindrical bore hole the pulse shape (time structure) at a position x can be determined from Fig. 5. The particle density exhibits infinitely steep gradients at the front and the trailing edge of the pulse. For a finite slit width Δx these slopes become finite.

The number of particles per pulse decreases proportionally to the pulse duration, for standard rotating disk choppers. At extreme slit positions the particle number of the microchopper is proportional to the pulse duration to the 1.5th power due to the curvature of the bore hole. The number of particles per pulse can be increased without increasing the overall pulse duration by employing a knife edge (or broad slit) which restricts only one side of the pulse while the other side is formed by the right hand side tip of the triangle in Fig. 3. In this geometry the pulse shape is slightly different from the one shown in Fig. 5. For the three-dimensional problem with a knife edge the number of particles per pulse can be approximated within a few percent by

$$n = \frac{\rho v d^3}{6R\omega} \left[1 - \frac{2}{d} \left(x + \frac{R^2\omega}{v} \right) \right]^{2.45}, \quad (2)$$

where ρ is the number of particles per volume in the beam.

IV. EXPERIMENT

At rotational frequencies below 100 Hz the magnetic suspension forces the rotor to rotate around an axis that is parallel to the bore hole axis. At a frequency of 106 Hz, however, this motion becomes unstable and precession motion begins to turn the rotor in the magnetic fields so that it ends up rotating around the axis with the largest moment of inertia. At slightly higher frequencies and in high vacuum the critical frequency is overcome and the rotation exhibits excellent stability with lateral vibrational amplitudes of less than 1/10 mm. The chosen rotor material withstands the tensile forces at 10 kHz. Operation of the rotor for several hours close to this frequency did not create any visible distortions of its shape.

The free-drift deceleration rate of the rotor in high vacuum ($< 10^{-6}$ mbar) is measured as $-\dot{\omega}/\omega = 10^{-5} \text{ s}^{-1}$.

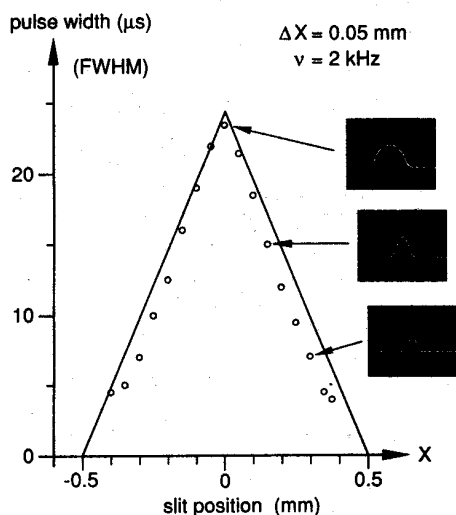


FIG. 6. Pulse width as a function of slit position at a rotation frequency of 2 kHz. The solid line indicates the calculated full width at half maximum pulse length for an infinitely narrow slit and a bore hole diameter of 1.0 mm. The solid circles are the measured full widths at half maximum of the pulses for the setup of Fig. 1 and a slit width of $\Delta x = 0.05$ mm. The three oscilloscope images on the right hand side show the pulse shape for the measurements indicated. At the extreme slit positions the intensity falls off rapidly.

It corresponds to a frequency decrease of less than 1% in 15 min. Thus, measurements for 10 min at 10 kHz, are broadened additionally by less than $0.5 \mu\text{s}$. The deceleration rate in high vacuum is more than two orders of magnitude larger than the one of a spinning sphere (2.5–4.5 mm in diameter).¹¹ It is entirely due to eddy currents (a) within the rotor and (b) in the tube and the SRG head, induced by the magnetic moment of the spinning rotor.

The measured pulse shapes and pulse durations are shown in Fig. 6. For these measurements we employ the setup of Fig. 1 with a Nicolet 1072 multichannel analyzer. We use a monochromatic helium atom beam from a room temperature Campargue-type nozzle¹² with a beam velocity of $v = 1800$ m/s, and a relative width of the velocity distribution of $\Delta v/v < 0.01$ [full width at half maximum (FWHM)]. A time resolving detector detects the helium atoms at a distance of 150 mm behind the rotor. The pulse dispersion at this position is negligible ($\Delta\tau < 0.8 \mu\text{s}$). The time resolution of the detector for the described nozzle beam is approximately $1.8 \mu\text{s}$ (FWHM).⁸

Due to these limitations to experimental resolution, the generated pulse lengths cannot be directly measured at a frequency of 10 kHz. They can, however, be predicted from the measurement at 2 kHz (Fig. 6): An upper limit of the pulse lengths at 10 kHz is given by dividing the time scale in Fig. 6 by a factor of 5. In fact the true pulse lengths

will be somewhat shorter due to the high pass behavior of the chopper.

The total number of particles in a pulse is small which results from both the small height and the curvature of the bore hole. For a pulse length of $1 \mu\text{s}$ at a frequency of 10 kHz and a room temperature nozzle beam, the transmitted volume per pulse is $V = n/\rho = 0.007 \text{ mm}^3$ [from Eq. (2)]. This low value is compensated by the high pulse repetition rate. With the high intensity He atom beam described above we estimate 10^5 atoms per pulse or 10^9 atoms per second.

In summary, we have developed and tested a neutral beam microchopper which resembles a miniature version of a neutron beam chopper. A magnetically suspended rotor, 5.6 mm diameter, rotates in vacuum. A cylindrical bore hole in the rotor perpendicular to the rotational axis chops the neutral beam. At a rotational frequency of 10 kHz the length of the generated pulses can be quickly adjusted between $5 \mu\text{s}$ and below $1 \mu\text{s}$ by positioning a slit in front of the rotor. For very small widths of this slit, the pulses exhibit steep particle density gradients at the front and trailing edges of the pulse. Due to a total diameter of the chopper set of less than 70 mm it can be employed in experiments where space is limited.

ACKNOWLEDGMENT

We wish to thank the machine shop of the IGV at the Forschungszentrum Jülich for the careful and precise manufacturing of the rotor.

- ¹E. Pöhlmann, R. Hüttel, and H. Knecht, *J. Phys. E.* **20**, 455 (1987).
- ²H. H. Sawin, D. D. Wilkinson, W. M. Chan, S. Smiriga, and R. P. Merrill, *J. Vac. Sci. Technol.* **14**, 1205 (1977).
- ³Y. Hirai, M. Shimatani, and S.-I. Hyodo, *J. Phys. E.* **13**, 251 (1980).
- ⁴G. Comsa, R. David, and B. J. Schumacher, *Rev. Sci. Instrum.* **52**, 789 (1981).
- ⁵H. Pauly and J. P. Toennies, in *Methods of Experimental Physics*, edited by B. Bederson and W. Fite (Academic, New York, 1986), Vol. 7A, p. 227ff.
- ⁶J. K. Fremerey, *J. Vac. Sci. Technol. A* **3**, 1715 (1985).
- ⁷V. F. Turchin, *Slow Neutrons*, Israel Program for Scientific Translations, (Sivan, Jerusalem, 1965), Chap. IV, Sec. 2.
- ⁸K. Kuhnke, R. David, K. Kern, and G. Comsa (in preparation).
- ⁹In the center of a rotating cylinder the tensile strain is $\sigma_{\text{max}} = 0.4125 \rho \omega R^2$ (density of the rotor material $\rho_{\text{C100}} \approx 8 \times 10^3 \text{ kg/m}^3$). Above and below the bore hole the strain has to be multiplied by the factor 3.2; *Dubbels, Taschenbuch für den Maschinenbau*, 15. Auflage (Springer, Berlin, 1986), p. 219 and 183.
- ¹⁰Particles are removed from the beam by hitting the inner surface of the bore hole at small angles. In scattering from technical surfaces, molecules are almost diffusely scattered even close to grazing incidence; F. C. Hurlbut, *J. Appl. Phys.* **28**, 844 (1957).
- ¹¹J. K. Fremerey, *Rev. Sci. Instrum.* **43** (10) 1413 (1972); **42**, 753 (1971).
- ¹²For the principle of the beam source, see R. Campargue, *J. Phys. Chem.* **88**, 4466 (1984). For the parameters of the source described here, see K. Kuhnke, Ph.D. thesis, Berichte des Forschungszentrums Jülich Jül-2490, 1991.